

Virtual Screening-Based Discovery and Mechanistic Characterization of the Acylthiourea MRT-10 Family as Smoothened Antagonists^[S]

Fabrizio Manetti, Helene Faure, Hermine Roudaut, Tatiana Gorojankina, Elisabeth Traiffort, Angele Schoenfelder, Andre Mann, Antonio Solinas, Maurizio Taddei, and Martial Ruat

Dipartimento Farmaco Chimico Tecnologico, Università degli Studi di Siena, Siena, Italy (F.M., A.S., M.T.); Centre National de la Recherche Scientifique, Unité Propre de Recherche-3294, Laboratoire de Neurobiologie et Développement, Institut de Neurobiologie Alfred Fessard IFR2118, Signal Transduction and Developmental Neuropharmacology Team, Gif-sur-Yvette, France (H.F., H.R., T.G., E.T., M.R.); and Laboratoire d'Innovation Thérapeutique, Centre National de la Recherche Scientifique, Unité Mixte de Recherche-7200, Université de Strasbourg, Illkirch, France (A.S., A.M.)

Received March 26, 2010; accepted July 27, 2010

ABSTRACT

The seven-transmembrane receptor Smoothened (Smo) is the major component involved in signal transduction of the Hedgehog (Hh) morphogens. Smo inhibitors represent a promising alternative for the treatment of several types of cancers linked to abnormal Hh signaling. Here, on the basis of experimental data, we generated and validated a pharmacophoric model for Smo inhibitors constituted by three hydrogen bond acceptor groups and three hydrophobic regions. We used this model for the virtual screening of a library of commercially available compounds. Visual and structural criteria allowed the selection of 20 top scoring ligands, and an acylthiourea, *N*-(3-benzamidophenylcarbamothioyl)-3,4,5-trimethoxybenzamide (MRT-10), was identified and characterized as a Smo antagonist. The cor-

responding acylurea, *N*-(3-benzamidophenylcarbamoyl)-3,4,5-trimethoxybenzamide (MRT-14), was synthesized and shown to display, in various Hh assays, an inhibitory potency comparable to or greater than that of reference Smo antagonists cyclopamine and *N*-((3*S*,5*S*)-1-(benzo[d][1,3]dioxol-5-ylmethyl)-5-(piperazine-1-carbonyl)pyrrolidin-3-yl)-*N*-(3-methoxybenzyl)-3,3-dimethylbutanamide (Cur61414). Focused virtual screening of the same library further identified five additional related antagonists. MRT-10 and MRT-14 constitute the first members of novel families of Smo antagonists. The described virtual screening approach is aimed at identifying novel modulators of Smo and of other G-protein coupled receptors.

Introduction

The Hedgehog (Hh) signaling pathway is involved in tissue growth and repair in the embryo and the adult. Synthesized as large precursor proteins, Hh ligands undergo autoproteolysis and lipid modifications of their biologically active aminoterminal domain. This soluble fragment mediates its action via a receptor complex containing two transmembrane proteins: Patched (Ptc) displaying a transporter-like structure and Smoothened (Smo) presumably belonging to the G protein-coupled receptor (GPCR) superfamily. The repres-

This work was supported by La Ligue contre le Cancer (Comité des Yvelines); l'Institut National du Cancer; l'Association pour la Recherche contre le Cancer [Grant 3850], l'Association Française contre les Myopathies [Grant 12181]; the French Agence Nationale de la Recherche [Grant 07-physio-010-04]; and The Neuropole de Recherche Francilien [Doctoral Fellowship 248890].

F.M. and H.F. contributed equally to this work.

Article, publication date, and citation information can be found at <http://molpharm.aspetjournals.org>.

doi:10.1124/mol.110.065102.

[S] The online version of this article (available at <http://molpharm.aspetjournals.org>) contains supplemental material.

ABBREVIATIONS: Hh, Hedgehog; Ptc, Patched; GPCR, G protein-coupled receptor; Smo, Smoothened; BCC, basal cell carcinoma; Cur61414, *N*-((3*S*,5*S*)-1-(benzo[d][1,3]dioxol-5-ylmethyl)-5-(piperazine-1-carbonyl)pyrrolidin-3-yl)-*N*-(3-methoxybenzyl)-3,3-dimethylbutanamide; Z''''', *N*-(4-chloro-3-(6-(dimethylamino)-1*H*-benzo[d]imidazol-2-yl)phenyl)-2,3-dihydrobenzo[b][1,4]dioxine-6-carboxamide; SAG, Smoothened agonist; DMSO, dimethyl sulfoxide; HEK, human embryonic kidney; IP, inositol phosphates; ShhN, N-terminal fragment of human Sonic hedgehog; AP, alkaline phosphatase; PBS, phosphate-buffered saline; DAPI, 4,6-diamidino-2-phenylindole; BC, Bodipy-cyclopamine; HBA, hydrogen-bond acceptor; HY, hydrophobic; MRT-24, *N*-(3-benzamidophenylcarbamothioyl)-3,4-dimethoxybenzamide; MRT-29, 4-methoxy-*N*-(3-(2-methylbenzamido)phenylcarbamothioyl)-3-nitrobenzamide; MRT-31, *N*-(3-(3-biphenylcarbonylthioureido)phenyl)furan-2-carboxamide; MRT-39, *N*-(3-(3-(3,4-dimethoxybenzoyl)thioureido)phenyl)furan-2-carboxamide; MRT-42, *N*-(5-(benzo[d]thiazol-2-yl)-2-methylphenylcarbamothioyl)-3,4-dimethoxybenzamide.

sion exerted by Ptc on Smo is relieved when Hh binds Ptc, which leads to a complex signaling cascade involving the transcription factors of the Gli family and to the activation of target genes, including Ptc and Gli themselves (Ruiz i Altaba et al., 2007; Hausmann et al., 2009; Simpson et al., 2009). Smo trafficking to the primary cilia from cytoplasmic vesicles has been proposed to be a key step for Hh transduction. Ptc is proposed to be localized to the cilia in the absence of its ligand and to inhibit signaling by excluding Smo. Thus, Smo translocation to the primary cilia upon Hh signaling might be followed by a second step leading to its activation, which has led to the proposition of a two-step mechanism of action for the activation process (Gerdes et al., 2009; Rohatgi et al., 2009; Wang et al., 2009b). Because Smo has been exclusively associated with synaptic vesicles in mossy fiber boutons in the hippocampus (Masdeu et al., 2007), it would be also important to determine whether this two-step mechanism of action is also observed for Smo transduction of Hh signaling in nerve brain terminal (Traiffort et al., 2010).

Dysregulation of the Hh pathway has been associated with several types of cancers. The inactivating mutations of Ptc observed in patients with Gorlin's syndrome have been linked to a higher incidence of basal cell carcinoma (BCC), medulloblastoma, and rhabdomyosarcomas. Oncogenic mutations of Smo have also been identified in both BCC and medulloblastoma (Scales and de Sauvage, 2009). These tumors are considered to be independent of Hh ligands because the pathway is constitutively activated. However, several types of cancers are considered to be dependent on the overproduction of Hh ligands. This is the case for those occurring from the gastrointestinal tract, lung, colon, pancreas, breast, and prostate and for melanoma (Mahindroo et al., 2009; Scales and de Sauvage, 2009).

Smo has been proposed as a molecular target for the action of antagonists aimed at blocking the Hh pathway and Smo inhibitors are candidate drugs for the treatment of cancers associated with dysfunction of Hh signaling. The natural and teratogenic compound cyclopamine blocks Hh signaling by directly binding Smo and slows down the growth of these tumors in various animal models (Taipale et al., 2000; Scales and de Sauvage, 2009; Simpson et al., 2009). When applied in vivo, cyclopamine also blocks stem cell proliferation in the mouse adult brain subventricular zone (Palma et al., 2005). However, it was recently proposed that cyclopamine and possibly another unrelated Smo antagonist may have non-specific effects on cell growth by acting on off-targets. They may mediate their effects on tumor growth by acting on the Hh pathway expressed in the stroma surrounding the tumor and not on the cells belonging to the tumor itself (Yauch et al., 2008; Tian et al., 2009). Cyclopamine has been tested for treating BCC in humans, and more potent and soluble derivatives are under development. *N*-((3*S*,5*S*)-1-(benzo[*d*][1,3]dioxol-5-ylmethyl)-5-(piperazine-1-carbonyl)pyrrolidin-3-yl)-*N*-(3-methoxybenzyl)-3,3-dimethylbutanamide (Cur61414) has also shown efficacy for treating BCC-like lesions in a mouse model but not in humans (Williams et al., 2003; Scales and de Sauvage, 2009). More recent clinical trials have been conducted with a novel small molecule Smo inhibitor for treating metastatic BCC and one case of medulloblastoma (Rudin et al., 2009; Von Hoff et al., 2009). However, in the latter, despite a rapid regression of the tumor and associated symptoms, resistance to the treatment occurred. A

Smo mutation altering its ability to respond to the inhibitor was proposed to be responsible for the observed resistance (Yauch et al., 2009). Hh blockade by a Smo antagonist has also been suggested to be a therapeutic approach to inhibit articular cartilage degeneration (Lin et al., 2009).

Therefore, the discovery of novel molecules aimed at inhibiting Smo has therapeutic interest and should help to further characterize the potential roles of Smo both in vitro and in vivo. Molecules with diverse structural features have been identified from high-throughput screening as Hh pathway inhibitors, and several of them target Smo (Mahindroo et al., 2009; Scales and de Sauvage, 2009). Such an approach requires intense screening efforts and is highly expensive. Virtual screening has become a major focus for the discovery of novel modulators of GPCRs. Because no three-dimensional structure of Smo has been reported so far, neither from experimental sources (i.e., NMR or X-ray crystallographic studies) nor from theoretical approaches (i.e., homology modeling and molecular dynamics simulations), we undertook a ligand-based virtual screening for new Smo antagonists. We first constructed and validated a Smo pharmacophore. Then, we applied a virtual screening procedure to select 20 compounds from the Asinex database. This approach resulted in the identification of MRT-10, a Smo antagonist displaying a unique acylthiourea scaffold. Finally, MRT-14, the corresponding acylurea derivative of MRT-10, was synthesized. In Hh cell-based assays, MRT-14 exhibited greater potency than MRT-10 comparable with that of reference Smo antagonists.

Materials and Methods

Drugs. Cyclopamine and Bodipy-cyclopamine were from Toronto Research Chemicals Inc. (North York, ON, Canada). SAG, Cur61414, and *N*-(4-chloro-3-(6-(dimethylamino)-1*H*-benzo[*d*]imidazol-2-yl)phenyl)-2,3-dihydrobenzo[*b*][1,4]dioxine-6-carboxamide (Z''') were synthesized as described previously (Martínez et al., 2006; Masdeu et al., 2006). ShhN was provided by Dr. D. Baker (Biogen Idec, Boston, MA). Other compounds selected from the virtual screening were from ASINEX (Rijswijk, The Netherlands), and their structures are shown in Table 2 and Supplemental Table 2. The structure of MRT-10 was confirmed by synthesis, and its biological activity evaluated on Hh assays was comparable with the purchased sample. Cur61414, SAG, and cyclopamine were dissolved in ethanol at a concentration of 10 mM. All other tested compounds were dissolved in DMSO at a concentration of 10 mM.

Preparation of *N*-(3-Benzamidophenylcarbamothioyl)-3,4,5-trimethoxybenzamide (MRT-10). A mixture of 3,4,5-trimethoxybenzoyl chloride and NH₄SCN in acetone was heated under reflux for 30 min. Then *N*-(3-aminophenyl)benzamide was added for 1 h. The reaction was poured into crushed ice with stirring; the solid collected and crystallized in hot MeOH gave MRT-10 (m.p. 164°C). ¹H NMR (300 MHz, CDCl₃) δ 12.69 (1 H, brd s), 9.03 (1 H, brd s), 8.24 (1 H, m), 7.93–7.89 (3 H, m) 7.63–7.42 (6 H, m), 7.10 (2 H, s), 3.96 (9 H, s). ¹³C NMR (75 MHz, DMSO, d₆) δ 179.9, 168.3, 166.5, 153.4, 142.5, 140.4, 139.1, 135.6, 132.5, 129.6, 129.2, 128.5, 127.5, 120.3, 119.1, 116.9, 107.2, 61.1, 57.1. C₂₄H₂₃N₃O₅S (molecular weight, 465) [electrospray/mass spectrometry] *m/z* 466 [M + H]⁺.

Preparation of *N*-(3-Benzamidophenylcarbamoyl)-3,4,5-trimethoxybenzamide (MRT-14). A mixture of 3,4,5-trimethoxybenzamide and oxalyl chloride in CH₂Cl₂ was refluxed for 16 h. The solvent was removed in vacuo, by adding toluene. Then, the crude acyl-isocyanate was dissolved in CH₃CN and *N*-(3-aminophenyl)benzamide was added. The reaction mixture was refluxed and the

resulting solid was filtered and crystallized in hot MeOH to yield MRT-14 as a white solid (m.p. 192°C). ^1H NMR (300 MHz, DMSO, d_6) δ 11.02 (2 H, m), 10.33 (1 H, brd s), 8.09–7.97 (3 H, m), 7.61–7.33 (8 H, m), 3.96 (9 H, s). $\text{C}_{24}\text{H}_{23}\text{N}_3\text{O}_6$ (molecular weight, 449) [electrospray/mass spectrometry] m/z 450 $[\text{M} + 1]^+$.

Structural Characterization of Compounds. The ^1H NMR (200 or 300 MHz), and ^{13}C NMR (50 or 75 MHz) spectra were performed in CDCl_3 or DMSO (d_6). The chemical shifts are given in parts per million with respect to CDCl_3 as the reference resonance. The melting points were performed on a Gallenkamp apparatus and were uncorrected.

Plasmids. The plasmids pRK5, pRK5- G_{15} , and pRK5-SP-myc-Smo encoding the mouse Smo sequence have been described previously (Masdeu et al., 2006) and are referred to in the text as pRK5, G_{15} , and mouse Smo, respectively.

Cell Culture and Transfection. HEK293 and C3H10T1/2 cells (American Type Culture Collection, Manassas, VA) were cultured in Dulbecco's modified Eagle's medium supplemented with 10% fetal calf serum (Invitrogen, Cergy-Pontoise, France). The Shh-light2 cells (from Prof. P.A. Beachy, Stanford University School of Medicine, Stanford, CA) were cultured in the same medium supplemented with 400 $\mu\text{g}/\text{ml}$ G-418 (Geneticin) and 150 $\mu\text{g}/\text{ml}$ Zeocin (Invitrogen). HEK293 cells were transiently transfected by electroporation using 4 μg of mouse Smo and 6 μg of pRK5 for Bodipy-cyclopamine binding and immunofluorescence or with 4 μg of mouse Smo supplemented with 4 μg of G_{15} and 2 μg of pRK5 for [^3H]inositol phosphates ([^3H]IP) formation. Controls with G_{15} or mouse Smo alone were performed in parallel experiments. The electroporated cells were distributed into six-well plates containing glass coverslips coated with 0.05 mg/ml poly-D-lysine (BD Bioscience, Le Pont De Claix, France) for Bodipy-cyclopamine binding and immunofluorescence experiments or 24-well plates for [^3H]IP analysis. These cell-based assays were performed 48 h after cell transfection.

Gli-Dependent Luciferase Reporter Assay. Shh-light2 cells stably incorporating the Gli-luc reporter and the prL-TK *Renilla reniformis* control described in (Taipale et al., 2000) were incubated for 40 h with ShhN (5 nM) and the studied compounds. Determination of luciferase activities was carried out using the Dual-Luciferase assay according to the manufacturer's instructions (Promega, Charbonnières-les-Bains, France). All presented data are firefly luciferase activity reported to the *R. reniformis* control activity. The MRT compounds did not modify significantly the *R. reniformis* activity at 3 μM .

Alkaline Phosphatase Assay. C3H10T1/2 cells were incubated for 6 days in the presence of SAG (0.1 μM) and the studied compounds. The cell-based bioassay was performed as described previously (Coulombe et al., 2004).

[^3H]IP Formation. Measurement of [^3H]IP accumulation was performed as described previously (Masdeu et al., 2006). Data are expressed as percentage Smo-induced IP response in the presence of G_{15} over the IP basal level. The latter corresponds to the inhibition of the Smo-induced IP response by 30 μM Cur61414. This response was not significantly different from the IP response observed in the presence of G_{15} alone. The [^3H]IP accumulation in G_{15} -transfected cells was not affected by 30 μM MRT-10 or Cur61414.

Bodipy-Cyclopamine Binding. The protocol was adapted from Chen et al. (2002a). Mouse Smo-transfected cells were fixed in 4% paraformaldehyde in phosphate-buffered saline (PBS) for 10 min, washed in PBS supplemented with 0.5% fetal calf serum and incubated for 2 h at 37°C in the same medium supplemented with Bodipy-cyclopamine (5 nM) and the studied compounds. After two washes in PBS-fetal calf serum, the cells were analyzed under a DMRXA2 fluorescence microscope (Leica Microsystems, Nanterre, France) equipped with a Photometric Cool-Snap camera (Roper Scientific, Ottobrunn, Germany) using Vectashield as mounting medium and DAPI for staining of the cell nuclei (Vector Laboratories, Paris, France). Bodipy (green) and DAPI (blue) signals were ana-

lyzed in three to four representative fields per coverslip (black and white photographs with 20 \times magnification, 1000 cells/field). Using Simple-PCI software (Hamamatsu Corporation, Massy, France), the fluorescence intensity of transfected cells determined in presence of BC (5 nM) alone or in the presence of the drugs, over the basal fluorescence measured in the absence of BC was quantified (Supplemental Table 3) and divided by the area occupied by the nuclei (DAPI staining) in the field. Data were expressed as percentage fluorescence intensity observed with BC alone.

Pharmacophore Determination and Virtual Screening. The chemical structures of diverse potent Hh inhibitors (Cur61414, Z''''', and related molecules shown in Supplemental Fig. 1) were used to generate the pharmacophoric model by means of the software Catalyst (Accelrys Inc., San Diego, CA). For this purpose, HipHop (common feature hypothesis generation), which is able to generate pharmacophoric models only by identification of the common chemical features shared by the molecules and their relative alignment to the common feature set (Barnum et al., 1996), was applied. Then, a conformational search was performed on each compound to build a representative family of conformational models to be used in turn for pharmacophore generation. Conformers were generated by application of the poling algorithm, and the best quality conformational analysis was implemented in the software Catalyst. Conformational diversity was emphasized by selection of the conformers that fell within a 20 kcal/mol range above the lowest-energy conformation. All the conformers of each compound were employed to derive a set of 10 pharmacophoric hypotheses (Supplemental Table 1). To enhance the probability of finding significant models, we have applied the following rules: 1) selection of the most potent molecules (Supplemental Fig. 1) to be included in the set, because the software pays particular attention to these molecules in the generation of the chemical feature space, and 2) maximization of the kinds (chemical groups) and relative positions (substitution pattern) of the chemical features (chemical groups) shared by the molecules, because the program recognizes the molecules as collections of chemical features, not as assemblies of atoms or bonds. The best-scored six-feature pharmacophore hypothesis was then used as a three-dimensional query to perform a database search to find structural motifs that fulfill the functional and spatial constraints imposed by the model. The Asinex Gold and Platinum Collection (<http://www.asinex.com/prod/gold.html>), containing approximately 400,000 compounds, was analyzed. The structure of compounds simultaneously mapping all the pharmacophore features with a fit value of 5.00 or higher (the maximum fit allowed by a six-feature pharmacophoric model is 6.00) were retained. The resulting library, composed of 525 entries, was further pruned to 20 entries on the basis of the fit value and the uniqueness of the molecular structure (Supplemental Table 2); i.e., among entries belonging to the same structural class, only the best scored compound was kept. These compounds were submitted to biological tests resulting in MRT-10 as a good hit compound. From its molecular structure, two substructures were designed (Supplemental Fig. 4). They have the ureido moiety and the central phenyl ring as common features, but differ in the presence of a terminal 6–5 heterocyclic moiety instead of a methoxyphenyl ring. They were used to perform two additional database searches.

Data Analysis. All experiments were carried out at least three times in triplicate or quadruplicate. Means and S.E.M. were calculated using Excel 2003 (Microsoft Corp., Redmond, WA). Curves were analyzed using Prism 4.03 (GraphPad Software, San Diego, CA). Data were fitted to sigmoidal dose-response curve (variable slope). The IC_{50} and Hill coefficient were calculated for each experiment, and the mean \pm S.E.M. are reported.

Results

Drug Discovery Approach. Several inhibitors of the Hh signaling pathway identified to date bind to the GPCR Smo at the level of its heptahelical domain. These include the

steroidal alkaloid extracted from corn lilies called cyclopamine, which is teratogenic, Cur61414, and several synthetic compounds widely used for blocking the Hh pathway both in vitro and in vivo (Scales and de Sauvage, 2009). Therefore, to allow the development of new Hh modulators, we have delineated a pharmacophore for Smo antagonists based on the structure of Cur61414, Z''', and several related molecules (Fig. 1 and Supplemental Fig. 1) for which the structures were available (Taipale et al., 2000; Chen et al., 2002b; Williams et al., 2003; Borzillo and Lippa, 2005). These molecules were selected for their potency as Smo antagonists and for the diversity of their chemical structures.

Owing to the lack of consistency in the reported biological data related to experimental variability in the biological responses analyzed by various laboratories, we felt it necessary to reinvestigate the antagonist properties of the lead molecules using established Hh cell-based assays under in-house homogenous conditions (Table 1, Fig. 2). The potency of cyclopamine, Cur61414, and Z''' was determined in Shh-light2 cells, which is an NIH3T3 cell line with a Gli-dependent firefly luciferase reporter widely used for identifying Hh inhibitors (Taipale et al., 2000). These cells were stimulated for 40 h with N-myristoylated Shh (ShhN) in the presence or absence of these drugs in parallel experiments. We also evaluated their ability to inhibit SAG (0.1 μ M)-induced differentiation of the mesenchymal pluripotent C3H10T1/2 cells into alkaline phosphatase-positive osteoblasts, a response that involves activation of Smo (Hyman et al., 2009). Z''' was found to be the most potent molecule in these assays (Table 1).

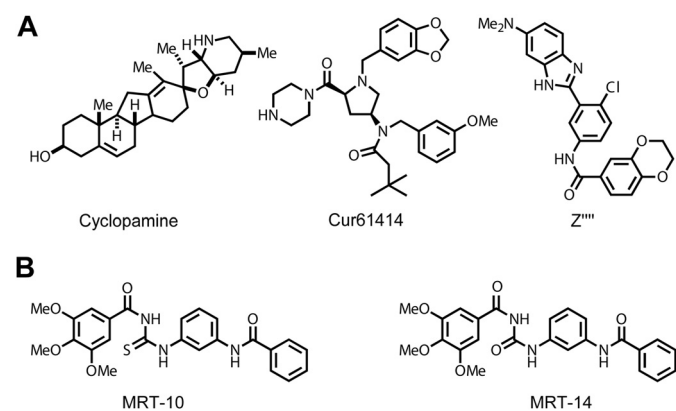


Fig. 1. Chemical structures of reference Smo antagonists (A). Structures of MRT-10 compound, identified from virtual screening, and MRT-14, its acylurea derivative (B).

TABLE 1

Compared activities of MRT-10, MRT-14, and reference Smo antagonists in different cell-based assays

IC₅₀ and Hill coefficient (n_H) values of the compounds were determined on Gli-dependent luciferase reporter activity induced by ShhN (5 nM) in Shh-light2 cells; AP activity induced by SAG (0.1 μ M) in C3H10T1/2 cells; constitutive activity of mouse Smo coexpressed with the α subunit of G₁₅ determined by IP accumulation in HEK293 cells; and BC binding to HEK293 cells transiently expressing mouse Smo. Data are the means \pm S.E.M. of two to five independent experiments.

Compounds	Shh-light2		C3H10T1/2		[³ H]IP		BC Binding	
	IC ₅₀	n_H	IC ₅₀	n_H	IC ₅₀	n_H	IC ₅₀	n_H
	μ M		μ M		μ M		μ M	
Cyclopamine	0.3 \pm 0.05	1.6 \pm 0.4	0.62 \pm 0.03	1.3 \pm 0.1	0.25 \pm 0.06	1.2 \pm 0.3	0.05 \pm 0.01	0.8 \pm 0.1
Cur61414	0.14 \pm 0.04	2.0 \pm 0.3	0.3 \pm 0.1	1.3 \pm 0.2	0.33 \pm 0.07	1.1 \pm 0.3	0.08 \pm 0.02	1.0 \pm 0.1
Z'''	0.09 \pm 0.05	1.8 \pm 0.1	0.029 \pm 0.007	1.1 \pm 0.1	0.12 \pm 0.01	1.0 \pm 0.1	0.011 \pm 0.001	1.4 \pm 0.3
MRT-10	0.64 \pm 0.15	2.0 \pm 0.4	0.9 \pm 0.2	1.3 \pm 0.2	2.5 \pm 1.1	0.9 \pm 0.2	0.5 \pm 0.2	1.0 \pm 0.3
MRT-14	0.16 \pm 0.07	2.1 \pm 0.3	0.13 \pm 0.05	1.2 \pm 0.1	0.6 \pm 0.2	1.1 \pm 0.2	0.12 \pm 0.03	1.3 \pm 0.3

Modeling and Virtual Library Screening. The best conformer analysis implemented in the Catalyst program was applied to each compound for collecting conformers with a range of 20 kcal/mol with respect to the global minimum that was used for building the best pharmacophoric model. This model was built up by three hydrogen bond acceptor (HBA1–3) groups and three hydrophobic (HY1–3) regions. Analysis of the superposition pattern of Z''' showed a perfect fit between the inhibitor and the pharmacophoric model (Fig. 3). For example, one of the dioxane oxygens of Z''' fills HBA1 perfectly; the oxygen atoms of the carbonyl moiety match HBA2, and one of the benzimidazole nitrogen atoms corresponds to the HBA3 feature of the model. Moreover, the phenyl ring of benzo-dioxane is superposed to the hydrophobic region HY1, the chloro-substituent on the central aromatic ring matches HY2, and the dimethylamino group is located in the spatial region occupied by HY3. Fitting of cyclopamine and Cur61414 to the pharmacophoric model is also shown in Supplemental Fig. 2.

Identification of the Acylthiourea MRT-10 Family of Smo Inhibitors. The Asinex Gold collection of diverse drug-like molecules was screened virtually for flexible fitting to the six-feature pharmacophore model of Smo. This in silico database search identified 525 compounds. After visual inspection of this library, 20 compounds were selected for experimental testing based on the following criteria: 1) high fit score, 2) molecular weight, and 3) chemical diversity.

These compounds were purchased and analyzed for both their antagonist properties in the Shh-light2 cell luciferase assay and their ability to inhibit SAG-induced differentiation of C3H10T1/2 cells using measurement of alkaline phosphatase activity (Supplemental Table 2). Among the tested molecules, MRT-10 (Fig. 1), an acylthiourea, behaved as an antagonist with potency similar to that of the reference compound Cur61414 (Fig. 2, Table 1). Then, we investigated the ability of MRT-10 to modify the constitutive activity of Smo coexpressed with the α subunit of the G₁₅ in HEK293 cells. This assay allows the analysis of the nontranscriptional activity of the Hh pathway and has been used for the characterization of the inverse agonist properties of cyclopamine and Cur61414 (Masdeu et al., 2006). In agreement with previous results, we showed that Cur61414 displays inverse agonist properties toward this response as measured by the decreased IP accumulation that occurred in these cells 30 min after the addition of the ligand (Fig. 4). Cur61414 inhibited the IP response (IC₅₀ = 0.33 μ M) in cells expressing both Smo and G₁₅ to a level comparable with that observed in

mock-transfected cells. Z''' also displays a full inverse agonism response ($IC_{50} = 0.12 \mu M$, Table 1). It is noteworthy that MRT-10 also inhibited the IP accumulation in a dose-dependent manner ($IC_{50} = 2.5 \mu M$). The inhibition of this response ($70 \pm 5\%$, $n = 3$) was partial (Fig. 4). Thus, MRT-10 has the capacity to abrogate the constitutive activity of Smo and should be considered as an inverse agonist for this response. These data also demonstrate that MRT-10 interacts with mouse Smo. MRT-10 and the other compounds presented in Table 1 have no significant inhibitory activity on the IP production in HEK cells transfected with G_{15} (Supplemental Fig. 5).

MRT-10 Binding to Cells Expressing Mouse Smo. To further investigate the binding properties of MRT-10 to Smo, we analyzed whether it can compete with Bodipy-cyclopamine, which interacts with Smo at the level of its heptahelical bundle (Chen et al., 2002b). First, we showed that Bodipy-cyclopamine bound to a subpopulation of HEK293 cells tran-

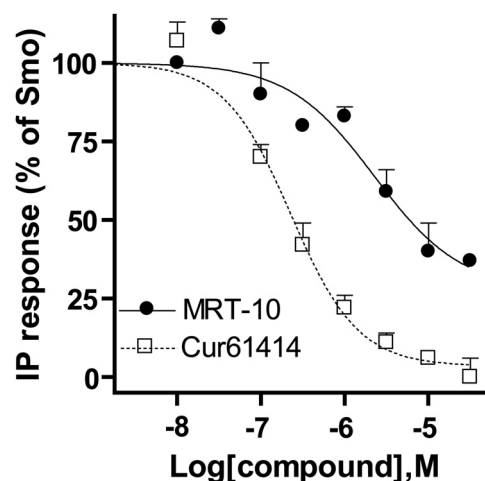


Fig. 4. Effects of Cur61414 and MRT-10 on Smo-induced IP response in HEK293 cells. HEK293 cells were transfected with G_{15} and mouse Smo and further incubated with increasing concentrations of Cur61414 and MRT-10 as described under *Materials and Methods*. The values used for concentration-response curves are expressed as a percentage of Smo-induced IP accumulation over basal level. They are representative of independent experiments ($n = 3-4$) and are the means \pm S.E.M. of triplicates.

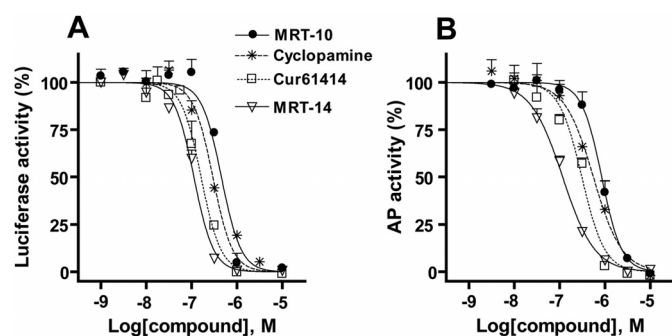


Fig. 2. Inhibition by MRT-10, MRT-14, Cur61414, and cyclopamine of ShhN-induced Gli-dependent luciferase activity in Shh-light2 cells (A) and SAG-induced differentiation of C3H10T1/2 cells (B). Inhibition curves were generated using increasing concentrations of MRT-10, MRT-14, Cur61414, and cyclopamine in the presence of ShhN (5 nM) (A) or SAG (0.1 μM) (B). The experiments were performed as described under *Materials and Methods*. The data shown are representative of independent experiments ($n = 3-10$) and are the means \pm S.E.M. of triplicates. The values are expressed as a percentage of the maximal response induced by ShhN or SAG, respectively.

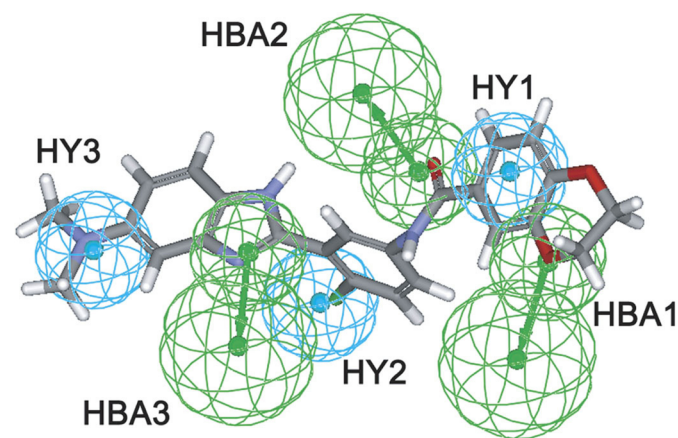


Fig. 3. Proposed pharmacophore model for Smo antagonists. Graphical representation of Z''' fitted to the pharmacophoric model for Smo antagonists. Pharmacophoric features are color coded: green for hydrogen bond acceptor groups (HBA1-3) and cyan for hydrophobic regions (HY1-3). HBA features are constituted by a smaller sphere accommodating the hydrogen bond acceptor group, by a directionality vector represented by an arrow, and by a larger sphere intended to allocate the hydrogen bond donor group of the target macromolecule. The atoms are color coded: gray, carbon; white, hydrogen; red, oxygen; and blue, nitrogen.

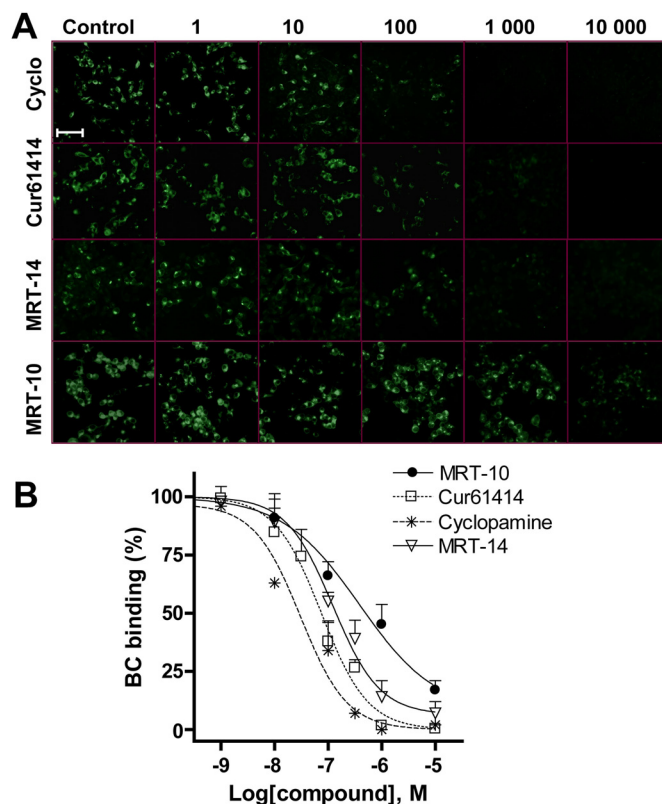


Fig. 5. Inhibition of Bodipy-cyclopamine binding to Smo by MRT-10, MRT-14, Cur61414, and cyclopamine. HEK293 cells were transiently transfected with mouse Smo and incubated with Bodipy-cyclopamine (5 nM) alone (Control) or in the presence of increasing concentrations (nanomolar) of the indicated compounds (Cyclo, cyclopamine). A, Bodipy-cyclopamine binding (green) is visualized using fluorescence microscopy in a representative field (150–200 cells shown; scale bar, 50 μM). B, the concentration-response curves for MRT-10, MRT-14, Cur61414, and cyclopamine were obtained by quantification of the Bodipy-cyclopamine fluorescence in three photographs for each coverslip as described in the *Material and Methods* and as exemplified in Supplemental Table 3. The values are expressed as a percentage of the fluorescence detected in control HEK293 cells incubated with Bodipy-cyclopamine alone. The data shown are the means of triplicates derived from a representative experiment of three.

siently transfected for expression of mouse Smo, as determined by fluorescence microscopy and immunostaining for the Smo protein, but did not bind to cells not expressing Smo (Supplemental Fig. 3). Then, the cells were incubated with 5 nM Bodipy-cyclopamine for 2 h in the presence or absence of various concentrations of MRT-10, cyclopamine, Z''', or Cur61414. At the end of the incubation, the cells were fixed and counterstained with DAPI. MRT-10 blocked Bodipy-cyclopamine binding to cells expressing mouse Smo in a dose-dependent manner (Fig. 5) with an $IC_{50} = 0.5 \mu M$, which was in good correlation with its IC_{50} in the Shh-light2 and AP assays (Table 1). Cyclopamine, Cur61414, and Z''' abrogated Bodipy-cyclopamine binding to cells expressing mouse Smo (Table 1). All together, these data demonstrate that MRT-10 binds to the Smo receptor at the level of the Bodipy-cyclopamine binding site.

Having established that MRT-10 behaves as a Smo antagonist and thus demonstrated the validity of our pharmacophoric model, we then screened the Asinex database for additional compounds featuring the phenylthiourea moiety. Among the thirty compounds of this second focused library, we identified five additional compounds [*N*-(3-benzamidophenylcarbamothioyl)-3,4-dimethoxybenzamide (MRT-24); 4-methoxy-*N*-(3-(2-methylbenzamido)phenylcarbamothioyl)-3-nitrobenzamide (MRT-29); *N*-(3-(3-biphenylcarbonylthioureido)phenyl)furan-2-carboxamide (MRT-31); *N*-(3-(3-(3,4-dimethoxybenzoyl)thioureido)phenyl)furan-2-carboxamide (MRT-39); *N*-(5-(benzo[d]thiazol-2-yl)-2-methylphenylcarbamothioyl)-3,4-dimethoxybenzamide (MRT-42)] that were able to inhibit significantly the responses at micromolar concentrations in the Shh-light2 cell and the AP assays (Table 2). The observed inhibition was in the same range or lower than with MRT-10. These compounds and MRT-10 did not modify by their own the basal response in the AP assays, indicating that they do not display agonist activity (Supplemental Fig. 6).

Synthesis and Characterization of the Acylurea MRT-14. Because the acylthiourea moiety seems to be an important fragment for receptor recognition, we decided to synthesize the corresponding acylurea derivative MRT-14 (Fig. 1), which can be obtained directly from MRT-10 by an oxidative desulfuration process. It is noteworthy that MRT-14 inhibited ShhN signaling in Shh-light2 cells in a dose-dependent manner with a 4-fold increased potency compared with MRT-10 ($IC_{50} = 0.16$ versus $0.64 \mu M$) (Table 1 and Fig. 2). The newly synthesized acylurea exhibited an inhibitory potency comparable with or greater than that of cyclopamine ($0.30 \mu M$) and Cur61414 ($0.14 \mu M$). A similar increase in potency for MRT-14 compared with MRT-10 was also observed in the AP assay ($IC_{50} = 0.13$ versus $0.90 \mu M$) and the IP response ($IC_{50} = 0.6$ versus $2.5 \mu M$, Table 1). The maximal inhibition of the IP response by MRT-14 ($70 \pm 5\%$, $n = 3$) was comparable with that observed for MRT-10, indicating that this compound is a partial inverse agonist. MRT-14 blocked Bodipy-cyclopamine binding to mouse Smo in a dose-dependent manner with an $IC_{50} = 0.12 \mu M$. Therefore, MRT-14, like MRT-10, displays Smo antagonist properties. These data also suggest that modifications of MRT-10 structure are amenable to the design of more potent compounds. It is noteworthy that the Hill coefficients of the dose response curves of cyclopamine, Cur61414, Z''', MRT-10, and MRT-14 were

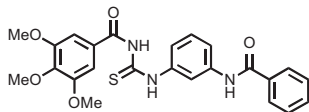
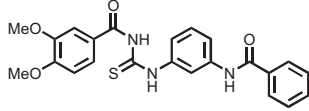
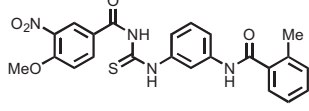
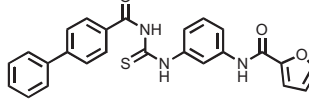
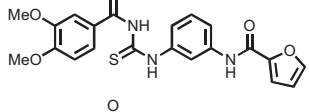
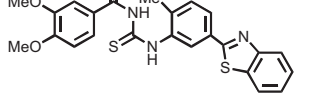
not different in all assays, suggesting a similar interaction of the various molecules with the receptor, whereas analysis of the slope of the concentration-response curves in the Shh-light2 luciferase assay indicated cooperativity ($n_H \approx 2$) (Table 1).

Pharmacophore Models of MRT-10 and MRT-14. MRT-10 and MRT-14 feature the following structural elements: an electron-rich phenyl ring (3,4,5-trimethoxy substituted) linked through an acylthiourea or an acylurea function, respectively, to a second phenyl bearing a phenyl carbamoyl residue. The superposition pattern of MRT-10 to the pharmacophore showed that one of the methoxy oxygen atoms of the ligand matches HBA1, the acylthiourea carbonyl oxygen represents HBA2, and the amide carbonyl oxygen is located within HBA3. The hydrophobic features are fitted by the aromatic rings of MRT-10 or MRT-14. The structural difference between MRT-10 and MRT-14 is also responsible for a slight different superposition to the pharmacophore (Fig. 6B). In fact, as a consequence of the transformation of the acylthiourea into an acylurea, the anchor point of HBA2 is located between the two carbonyl groups of MRT-14, thus allowing it to make a bifurcated hydrogen bond involving the oxygen atoms of both carbonyl groups and sharing the pro-

TABLE 2

Comparison of the inhibition induced by MRT compounds on ShhN-induced Gli-dependent luciferase activity in Shh-light2 cells and SAG-induced differentiation of C3H10T1/2 cells

The structure of MRT compounds identified in the first and second virtual library screening procedure are shown. The values correspond to percentage inhibition of the luciferase activity induced by ShhN (5 nM) in the presence of $3 \mu M$ concentrations of each compound analyzed in the Shh-light2 assay. The values correspond to percentage inhibition of AP activity induced by SAG ($0.1 \mu M$) in the presence of $10 \mu M$ of each compound analyzed in C3H10T1/2 cell differentiation assay. Data are the means \pm S.E.M. of at least three independent experiments.

Structure	Compound	Inhibition	
		Shh-light2	C3H10T1/2
		%	
	MRT-10	96 ± 1	96 ± 4
	MRT-24	71 ± 7	45 ± 8
	MRT-29	65 ± 4	36 ± 4
	MRT-31	49 ± 6	28 ± 6
	MRT-39	44 ± 2	49 ± 11
	MRT-42	77 ± 2	78 ± 2

jecting point of HBA2 as a common hydrogen bond acceptor counterpart.

Although MRT-10 and Z''' apparently display different structures such as an additional central carbamoyl fragment present in MRT-10 with respect to Z''', the two compounds fit well with the pharmacophoric model, the six features being satisfied by different functional groups. The structures of MRT-10 and MRT-14 are relatively easy to assemble, and variations on the three aromatic core are amenable to cognate chemistry. Because we have already identified five additional antagonists displaying the acylthiourea moiety, it can be anticipated that other derivatives of MRT-10 and MRT-14 displaying Smo antagonist properties will be obtained. Indeed, exchanging the sulfur with an oxygen atom, a better hydrogen bond acceptor, from MRT-10 to MRT-14, respectively, has already led to an increase of the antagonist potency.

Discussion

Thus, this work highlights the mainstream use of virtual screening protocols based on a pharmacophore for the identification of compound leads for Smo antagonists. On the basis of a pharmacophore for Smo ligands, we have here identified and characterized the mechanism of action of

MRT-10, an acylthiourea, and MRT-14, its acylurea derivative. They represent new leads that expand the chemical domain of Smo inhibitors. Although the crystal structures for the $\beta 1/\beta 2$ -adrenergic receptors and rhodopsin, three members of the GPCR family, have been obtained (Lodowski et al., 2009; Rosenbaum et al., 2009), there are few data describing the identification of new compound leads for GPCRs based on homology modeling of the putative ligand binding site. This site is proposed to be located within the heptahelical bundle of these proteins, which displays some structural conservation (Schalon et al., 2008). Homology model-based virtual screening using ligand docking and target-based scoring have encountered limited success for the identification of mGluR5 or melanin-concentrating hormone receptor modulators (Cavasotto et al., 2008; Radestock et al., 2008). The development of a proper pharmacophore model may be limited not only by accurate pharmacological data from known reference lead molecules but also by the conformational flexibility of GPCRs that might adopt multiple conformations linked to the activation process.

In the case of Smo, this intrinsic plasticity is presumably more complex than originally thought for GPCRs. Smo is proposed to act as a dimer, to be in active and inactive forms linked to Hh signaling, and to be differentially modulated by antagonists within cytoplasmic vesicles or at the primary cilia (Zhao et al., 2007; Rohatgi et al., 2009; Scales and de Sauvage, 2009; Wang et al., 2009b; Wilson et al., 2009). Moreover, agonists such as SAG derivatives and antagonists such as SANT-1 have been proposed to act in an allosteric manner on Smo, suggesting that multiple binding sites for Smo modulators exist at the level of the transmembrane domains (Chen et al., 2002b; Rominger et al., 2009). How Smo is regulated and whether Smo is modulated by an endogenous ligand remains unknown. However, allosteric ligands acting at the level of the heptahelical domain of GPCRs have been characterized recently and represent a novel therapeutic strategy (Conn et al., 2009; Wang et al., 2009a). MRT-10 and MRT-14 block Bodipy-cyclopamine binding to mouse Smo, suggesting that both molecules are acting at the same site or at allosteric sites. Site-directed mutagenesis and molecular modeling studies have allowed the identification of allosteric binding pockets for modulators of GPCRs (Petrel et al., 2004; Simpson et al., 2010). This approach together with binding and functional assays should help to further delineate the mechanism of action of Smo modulators.

In conclusion, we report here a successful virtual screening approach in which we identified and characterized MRT-10 and MRT-14 compounds as novel high-affinity Smo antagonists. These molecules, or more potent Smo inhibitors chemically derived from MRT-10 and MRT-14 that we are currently developing, should help to further understand Smo regulation and its interaction with accessory proteins both in vitro and in vivo. Moreover, our work has important implications for developing novel drugs for cancer therapy.

Acknowledgments

We thank Dr. S. O'Regan for critical reading of the manuscript.

References

- Barnum D, Greene J, Smellie A, and Sprague P (1996) Identification of common functional configurations among molecules. *J Chem Inf Comput Sci* 36:563–571.

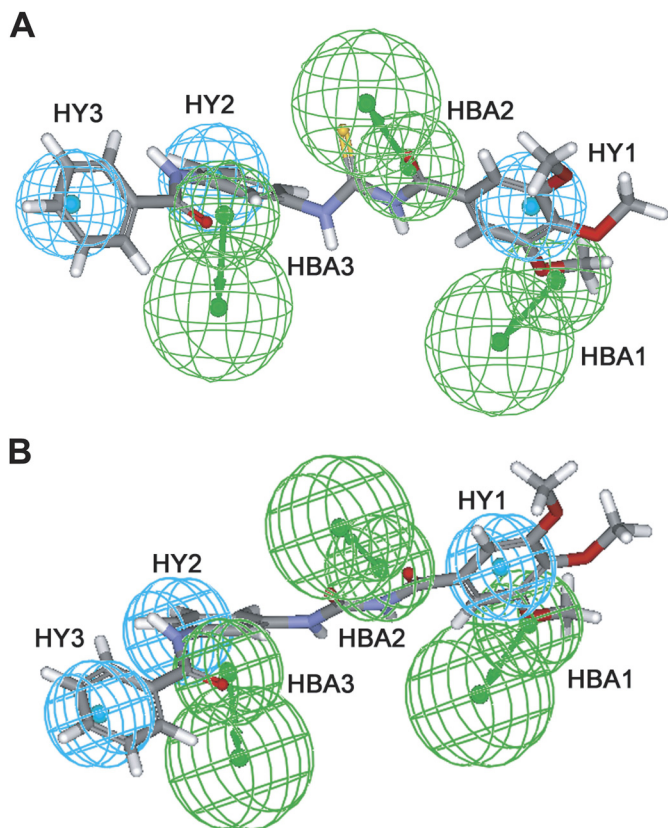


Fig. 6. Pharmacophore model for MRT-10 and MRT-14. Graphical representation of MRT-10 (A) and MRT-14 (B) fitted to the proposed pharmacophoric model for Smo antagonists. Pharmacophoric features are color coded: green for hydrogen bond acceptor groups (HBA1–3) and cyan for hydrophobic regions (HY1–3). HBA features are constituted by a smaller sphere accommodating the hydrogen bond acceptor group, by a directionality vector represented by an arrow, and by a larger sphere intended to allocate the hydrogen bond donor group of the target macro-molecule. The atoms are color coded: gray, carbon; white, hydrogen; red, oxygen; blue, nitrogen; yellow, sulfur.

- Borzillo GV and Lippa B (2005) The Hedgehog signaling pathway as a target for anticancer drug discovery. *Curr Top Med Chem* **5**:147–157.
- Cavasotto CN, Orry AJ, Murgolo NJ, Czarniecki MF, Kocsi SA, Hawes BE, O'Neill KA, Hine H, Burton MS, Voigt JH, et al. (2008) Discovery of novel chemotypes to a G-protein-coupled receptor through ligand-steered homology modeling and structure-based virtual screening. *J Med Chem* **51**:581–588.
- Chen JK, Taipale J, Cooper MK, and Beachy PA (2002a) Inhibition of Hedgehog signaling by direct binding of cyclopamine to Smoothened. *Genes Dev* **16**:2743–2748.
- Chen JK, Taipale J, Young KE, Maiti T, and Beachy PA (2002b) Small molecule modulation of Smoothened activity. *Proc Natl Acad Sci USA* **99**:14071–14076.
- Conn PJ, Christopoulos A, and Lindsley CW (2009) Allosteric modulators of GPCRs: a novel approach for the treatment of CNS disorders. *Nat Rev Drug Discov* **8**:41–54.
- Coulombe J, Traiffort E, Loulier K, Faure H, and Ruat M (2004) Hedgehog interacting protein in the mature brain: membrane-associated and soluble forms. *Mol Cell Neurosci* **25**:323–333.
- Gerdes JM, Davis EE, and Katsanis N (2009) The vertebrate primary cilium in development, homeostasis, and disease. *Cell* **137**:32–45.
- Hausmann G, von Mering C, and Basler K (2009) The hedgehog signaling pathway: where did it come from? *PLoS Biol* **7**:e1000146.
- Hyman JM, Firestone AJ, Heine VM, Zhao Y, Ocasio CA, Han K, Sun M, Rack PG, Sinha S, Wu JJ, et al. (2009) Small-molecule inhibitors reveal multiple strategies for Hedgehog pathway blockade. *Proc Natl Acad Sci USA* **106**:14132–14137.
- Lin AC, Seeto BL, Bartoszko JM, Khoury MA, Whetstone H, Ho L, Hsu C, Ali SA, Ali AS, and Alman BA (2009) Modulating hedgehog signaling can attenuate the severity of osteoarthritis. *Nat Med* **15**:1421–1425.
- Lodowski DT, Angel TE, and Palczewski K (2009) Comparative analysis of GPCR crystal structures. *Photochem Photobiol* **85**:425–430.
- Mahindroo N, Punchihewa C, and Fujii N (2009) Hedgehog-Gli signaling pathway inhibitors as anticancer agents. *J Med Chem* **52**:3829–3845.
- Martínez MC, Larbret F, Zobairi F, Coulombe J, Debili N, Vainchenker W, Ruat M, and Freyssinet JM (2006) Transfer of differentiation signal by membrane microvesicles harboring hedgehog morphogens. *Blood* **108**:3012–3020.
- Masdeu C, Bernard V, Faure H, Traiffort E, and Ruat M (2007) Distribution of Smoothened at hippocampal mossy fiber synapses. *Neuroreport* **18**:395–399.
- Masdeu C, Faure H, Coulombe J, Schoenfelder A, Mann A, Brabet I, Pin JP, Traiffort E, and Ruat M (2006) Identification and characterization of Hedgehog modulator properties after functional coupling of Smoothened to G15. *Biochem Biophys Res Commun* **349**:471–479.
- Palma V, Lim DA, Dahmane N, Sánchez P, Brionne TC, Herzberg CD, Gitton Y, Carleton A, Alvarez-Buylla A, and Ruiz i Altaba A (2005) Sonic hedgehog controls stem cell behavior in the postnatal and adult brain. *Development* **132**:335–344.
- Petrel C, Kessler A, Dauban P, Dodd RH, Rognan D, and Ruat M (2004) Positive and negative allosteric modulators of the Ca^{2+} -sensing receptor interact within overlapping but not identical binding sites in the transmembrane domain. *J Biol Chem* **279**:18990–18997.
- Radestock S, Weil T, and Renner S (2008) Homology model-based virtual screening for GPCR ligands using docking and target-biased scoring. *J Chem Inf Model* **48**:1104–1117.
- Rohatgi R, Milenkovic L, Corcoran RB, and Scott MP (2009) Hedgehog signal transduction by Smoothened: pharmacologic evidence for a 2-step activation process. *Proc Natl Acad Sci USA* **106**:3196–3201.
- Rominger CM, Bee WL, Copeland RA, Davenport EA, Gilmartin A, Gontarek R, Hornberger KR, Kallal LA, Lai Z, Lawrie K, et al. (2009) Evidence for allosteric interactions of antagonist binding to the smoothened receptor. *J Pharmacol Exp Ther* **329**:995–1005.
- Rosenbaum DM, Rasmussen SG, and Kobilka BK (2009) The structure and function of G-protein-coupled receptors. *Nature* **459**:356–363.
- Rudin CM, Hann CL, Laterra J, Yauch RL, Callahan CA, Fu L, Holcomb T, Stinson J, Gould SE, Coleman B, et al. (2009) Treatment of medulloblastoma with hedgehog pathway inhibitor GDC-0449. *N Engl J Med* **361**:1173–1178.
- Ruiz i Altaba A, Mas C, and Stecca B (2007) The Gli code: an information nexus regulating cell fate, stemness and cancer. *Trends Cell Biol* **17**:438–447.
- Scales SJ and de Sauvage FJ (2009) Mechanisms of Hedgehog pathway activation in cancer and implications for therapy. *Trends Pharmacol Sci* **30**:303–312.
- Schalch C, Surgand JS, Kellenberger E, and Rognan D (2008) A simple and fuzzy method to align and compare druggable ligand-binding sites. *Proteins* **71**:1755–1778.
- Simpson F, Kerr MC, and Wicking C (2009) Trafficking, development and hedgehog. *Mech Dev* **126**:279–288.
- Simpson LM, Taddese B, Wall ID, and Reynolds CA (2010) Bioinformatics and molecular modelling approaches to GPCR oligomerization. *Curr Opin Pharmacol* **10**:30–37.
- Taipale J, Chen JK, Cooper MK, Wang B, Mann RK, Milenkovic L, Scott MP, and Beachy PA (2000) Effects of oncogenic mutations in Smoothened and Patched can be reversed by cyclopamine. *Nature* **406**:1005–1009.
- Tian H, Callahan CA, DuPree KJ, Darbonne WC, Ahn CP, Scales SJ, and de Sauvage FJ (2009) Hedgehog signaling is restricted to the stromal compartment during pancreatic carcinogenesis. *Proc Natl Acad Sci USA* **106**:4254–4259.
- Traiffort E, Angot E, and Ruat M (2010) Sonic Hedgehog signaling in the mammalian brain. *J Neurochem* **113**:576–590.
- Von Hoff DD, LoRusso PM, Rudin CM, Reddy JC, Yauch RL, Tibes R, Weiss GJ, Borad MJ, Hann CL, Brahmer JR, Mackey HM, Lum BL, Darbonne WC, Marsters JC, Jr., de Sauvage FJ, and Low JA (2009) Inhibition of the hedgehog pathway in advanced basal-cell carcinoma. *N Engl J Med* **361**:1164–1172.
- Wang L, Martin B, Brennen R, Luttrell LM, and Maudsley S (2009a) Allosteric modulators of g protein-coupled receptors: future therapeutics for complex physiological disorders. *J Pharmacol Exp Ther* **331**:340–348.
- Wang Y, Zhou Z, Walsh CT, and McMahon AP (2009b) Selective translocation of intracellular Smoothened to the primary cilium in response to Hedgehog pathway modulation. *Proc Natl Acad Sci USA* **106**:2623–2628.
- Williams JA, Guicherit OM, Zaharian BI, Xu Y, Chai L, Wichterle H, Kon C, Gatchalian C, Porter JA, Rubin LL, et al. (2003) Identification of a small molecule inhibitor of the hedgehog signaling pathway: effects on basal cell carcinoma-like lesions. *Proc Natl Acad Sci USA* **100**:4616–4621.
- Wilson CW, Chen MH, and Chuang PT (2009) Smoothened adopts multiple active and inactive conformations capable of trafficking to the primary cilium. *PLoS One* **4**:e5182.
- Yauch RL, Dijkgraaf GJ, Aliche B, Januario T, Ahn CP, Holcomb T, Pujara K, Stinson J, Callahan CA, Tang T, et al. (2009) Smoothened mutation confers resistance to a Hedgehog pathway inhibitor in medulloblastoma. *Science* **326**:572–574.
- Yauch RL, Gould SE, Scales SJ, Tang T, Tian H, Ahn CP, Marshall D, Fu L, Januario T, Kallop D, et al. (2008) A paracrine requirement for hedgehog signalling in cancer. *Nature* **455**:406–410.
- Zhao Y, Tong C, and Jiang J (2007) Hedgehog regulates smoothened activity by inducing a conformational switch. *Nature* **450**:252–258.

Address correspondence to: Martial Ruat, Centre National de la Recherche Scientifique, UPR-3294, Laboratoire de Neurobiologie et Développement, Institut de Neurobiologie Alfred Fessard IFR 2118, Signal Transduction and Developmental Neuropharmacology team, 1 Avenue de la Terrasse, F-91198, Gif-sur-Yvette, France. E-mail: ruat@inaf.cnrs-gif.fr
